Indian Journal of Radio & Space Physics
Vol 47, September-December 2018, pp 42-48

Dual-band perfect meta material absorber with polarization independence and wide incidence angle

Kanwar Preet Kaur* & Trushit Upadhyaya

Department of Electronics & Communication Engineering, Chandubhai S Patel Institute of Technology, Charotar University of Science & Technology, Changa, Anand 388 421, India

Received 08 July 2017

A dual-band perfect meta-material absorber based on closed ring resonator structures (CRRs) with polarization independence and wide incidence angle stability is designed, simulated and measured. The absorber unit cell is composed of FR4 dielectric substrate sandwiched between the CRR and ground metal plane. The optimized design is numerically simulated to obtain two absorption peaks of around 99.66% at 1.98 GHz and 99.05% at 2.59 GHz. The proposed absorber structure exhibits absorption of above 99% for all polarization angle variations. The effect of variations in oblique angle under TE and TM mode configuration and loss tangent on absorption efficiency is presented to support the efficacy of the design. The numerical computation of design with a different dielectric material is performed to provide comparative result. The absorber structure is tested using waveguide measurement method which could be utilized for the absorption of the ambient UMTS band frequencies. The experimental results show fair agreement with the numerically simulated results.

Keywords: Closed ring resonators, Meta material absorbers, Dual-Band absorber, Polarization

1 Introduction

The need of thin, small and multiband/broad absorber at microwave to infrared frequencies has initiated the research in the direction of meta material inspired absorbers. An electromagnetic (EM) absorber is a passive device, capable of restraining the incident EM reflection and transmission of an EM wave. The exotic properties of meta materials (MTMs) such as negative permittivity, negative permeability and negative refraction[1-3] have given rise to many metamaterial based potential applications some of them are super lens[4,5], antenna[6,7], cloaking device[8], sensors[9,10] and EM energy harvesting[11,12]. Meta material absorbers (MMAs) are usually devised by the periodic arrangement of the unit cells. The unit cell acts as atoms present in naturally existing materials and the dimensions of these unit cells must be less than one-fourth of the working wavelength ($\lambda/4$)[13] in order that metamaterial operates as natural materials. In absorbers, unit cell are composed of dielectric which is sandwich between resonators and metal ground plane. The shaped resonators either split ring resonators (SRRs)[15] or closed ring resonators (CRRs)[16] with bottom metal plate give rise to electric and magnetic responses simultaneously as the EM wave is incident on the MMA surface.

Absorption is maximized by reducing the reflection from and transmission through the absorber structure. By matching the impedance of the absorber structure to the free space impedance the reflection from the structure is minimized. This impedance matching takes place when the effective permittivity, $\varepsilon(\omega)$, of the structure becomes equal to its effective permeability, $\mu(\omega)$, and a large imaginary component of the effective refractive index ($n(\omega) = \sqrt{\varepsilon(\omega)\mu(\omega)}$) is obtained at certain resonance frequency. Under this condition the real component of the effective impedance ($Z(\omega) = \sqrt{\mu(\omega)/\varepsilon(\omega)}$) becomes nearly equal to unity while making imaginary component as near zero[14].

The first MMA was proposed in the year 2008 by N. I. Landy[15] and the design was based on split ring resonators (SRRs). Since then, many MMA designs have been proposed based on SRR as well as based on CRR. The MMAs design presented in this paper is based on two distinct concentric CRRs which is simulated using full wave High Frequency Structure Simulator (HFSS) software. The outer ring is an octagonal ring for the absorption of EM wave centered at 1.98 GHz and inner ring is a rotated

*Corresponding author (Email: kanwarpreet27@gmail.com)

square ring for the absorption of 2.59 GHz band. The outer octagonal ring has larger electrical length which helps in providing reduced absorption frequency and polarization insensitivity is achieved due its 8-fold rotating symmetry. Further, the second absorption band is achieved at high frequency with polarization independence from a rotated square ring placed inside octagonal ring. The concentric CRR[16-20] designs are selected because of their folding symmetry which eventually yields in polarization insensitivity and other reason being ease in fabrication. The proposed absorber was designed for the absorption of ambient UMTS frequency bands (frequencies used by 3G wireless networks) covering L-band and lower S-band frequencies. Thus, the proposed absorber could be used for shielding RF electronic components or systems against EMI/EMC interventions. Most of the MMAs designs reported so far are based on mid S-band to X-band frequencies[20-24] (Table 1). The reason for such frequency selection is the size of the fabricated sample which is inversely proportional to the target frequency in case of free space measurement method. The sample size required for the free space measurement of the proposed MMA is found to be greater than ~1.5m. Such extremely large sample requirement makes free space measurement method impractical for testing proposed MMA. Hence, the waveguide measurement method is selected for testing proposed absorber where the required sample size is same as that of the inner dimension of the waveguide. The simulated results of return loss, effective normalized impedance, electric field distribution and surface current distributions were exhibited to support the efficacy of the proposed MMA design along with the measured results. Furthermore, numerical computations are carried out for the variations in loss tangents and number of unit cell with replacement of FR4 with a novel substrate material— neoprene rubber. The simulated absorption efficiency was obtained as 99.66% and 99.05% with return loss of 24.62 dB & 20.24 dB at 1.98 GHz & 2.59 GHz, respectively.

2 Proposed Absorber Design

Unit cell of the proposed absorber design consists of a substrate over which CRRs are engraved and the bottom side is terminated with a metal plate. The geometry of the proposed absorber design is depicted in Fig. 1. The top metal plate contains two distinct concentric CRRs; an outer octagonal resonator and an inner rotated square resonator. These ring resonators acts as electric ring resonators (ERRs) since they strongly coupled to the incident electric field and excite relatively ineffectively to the magnetic response as a consequence generating electric responses at the resonance frequencies. Meanwhile, the magnetic coupling occurs between the two CRRs and ground plate when the CRRs are combined with the metal ground plate. This magnetic coupling generates anti-parallel currents which in-turn results

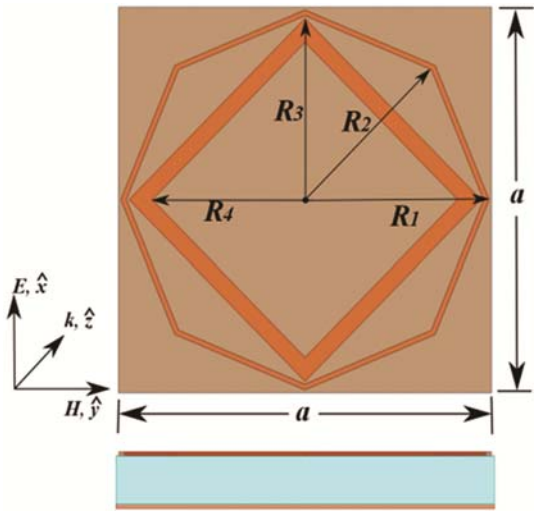

Fig. 1 — Proposed absorber structure geometries with concentric CRRs rings.

Table 1 — The recent reported Concentric CRR based microwave MMA.

Ref's	MMA Type	Unit Cell dimension (mm)	Concentric CRR shapes	Frequencies (GHz)	Absorption Efficiency (%)	Substrate Material
[18]	Triple band	14×14×1	Rotated square	4.84, 8.06 & 11.28	99.9, 97.9 & 97.8	FR4
[19]	Quad band	11×11×1.4	Square	3.54, 6.15, 8.42, & 12.9	> 97	FR4 with loss tangent=0.03
[20]	Dual band	10×10×1	Circular & Square	5.5 & 8.9	99.8 & 99.97	FR4
[28]	Broad band	4.2×4.2×1	Octagons	19.9 to 31.23	> 90	Foam
[29]	Penta band	10×10×1	Circular	5.28, 7.36, 9.52, 12.64 & 16.32	92.03, 90.46, 95.1, 91.65 & 91.1	FR4
Suggested MMA	Dual band	27.4×27.4×2.4	Rotated Octagon & Rotated Square	1.98 & 2.59	99.66 & 99.05	FR4
				2.05 & 2.71	97.26 & 94.17	Neoprene Rubber

in magnetic response. Thus, by changing the geometrical parameters electric and magnetic response could be changed simultaneously, thereby matching absorber structure impedance to the free space impedance[15].

Two distinct concentric CRRs of the proposed dual band MMA are imprinted on 2.4 mm thick FR4 dielectric substrate which is terminated with a copper plate. The copper sheet used for simulation has thickness of 0.035 mm and conductivity of 5.8×10^7 S/m. The relative permittivity and dielectric loss tangent of substrate are selected as 4.4 and 0.02 respectively. The geometrical dimensions of the absorber are optimized to the following values: a=27.4 mm, R_1=13.5 mm, R_2=13.1 mm, R_3=12.9 mm and R_4=11.2 mm. In simulation, the return loss parameter is obtained by applying periodic boundary conditions with floquet ports. The electric and magnetic fields are set at x-axis and y-axis direction, respectively, with EM wave propagating along z-axis direction. The absorber thickness calculated at the lower absorption frequency is approximately as $\lambda_0/60$.

3 Simulated Results and Analysis

The absorption efficiency is calculated from the following formula: $A(\omega)=1-R(\omega)-T(\omega)$. $R(\omega)$ and $T(\omega)$ are known as reflectance and transmittance respectively. They are related to the return loss and insertion loss in the manner as follows: $R(\omega)=|S_{11}(\omega)|^2$ and $T(\omega)=|S_{21}(\omega)|^2$. Theoretically, $S_{21}(\omega)$ is zero since the absorber structure is shielded with bottom metal plate having thickness greater than the penetration depth of targeted microwave frequencies. Practically, $S_{21}(\omega)$ was found to be approximately zero. The simulated results depicting all the three parameters are shown in Fig. 2. It should be noted that two absorption peaks were obtained at frequencies of 1.98 GHz and 2.59 GHz where return loss droped to a minimum value of 24.62 dB and 20.24 dB indicating that the effective impedance of the absorber matches the free space impedance. The absorption efficiencies at the respective dual frequencies are 99.66% and 99.05%.

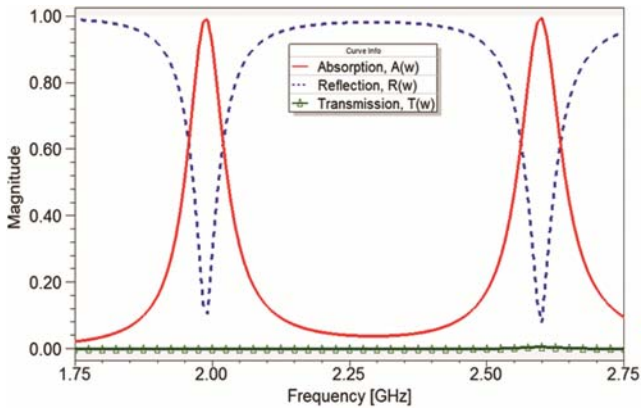

Fig. 2 — Simulated result depicting comparison of Absorption, reflection and transmission.

The effective normalized impedance of the proposed absorber is retrieved from the below mentioned retrieval algorithm[25] and the numerically retrieved normalized effective Z-parameter is shown in Fig. 3.

$$z = \sqrt{\frac{(1+S_{11})^2-S_{21}^2}{(1-S_{11})^2-S_{21}^2}} \quad \ldots (1)$$

It is observed from Fig. 3 that the real component of the normalized effective impedance roughly approaches to unity, whereas the imaginary component drops to a zero attaining impedance matching of absorber structure to the free space.

To better understand the physics behind the proposed dual-band MMA the surface current distribution and electric field distribution are discussed in details. Both the distributions are plotted separately for lower and higher absorption frequencies which are shown in Fig. 4 and Fig. 5 respectively. Figs 4(a),(b) and Figs 5(a),(b) illustrate the surface current distribution on top and bottom plane of the proposed MMA. It evident from these results that strong symmetric and anti-symmetric circular surface current loops are generated due to the coupling of CRRs with one another and with the dielectric spacer and ground plane for both the lower and higher absorption frequencies. By comparing current distribution graphs for both the frequencies it is observed that the surface current is strongly associated with the outer loop hence maximum

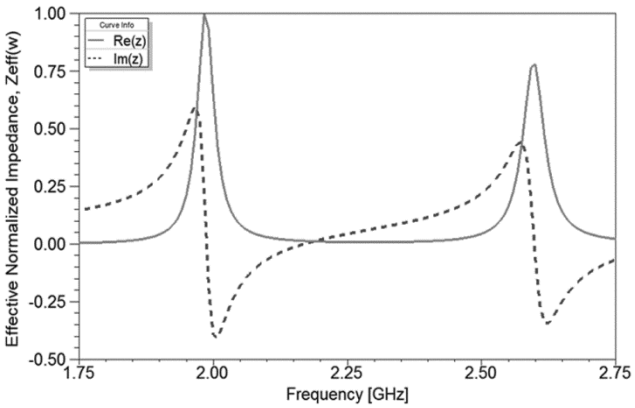

Fig. 3 — Retrieved effective normalized impedance

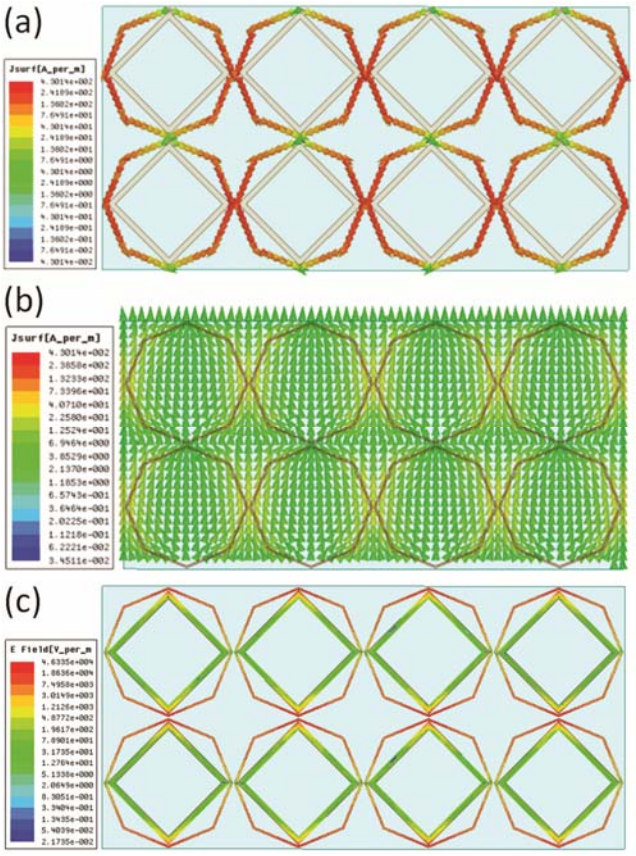

Fig. 4 — Calculated electrical parameters at low absorption frequency of 1.98 GHz: (a) Current distribution on top plane of the MMA, (b) current distribution on bottom plane of the MMA and (c) electric field distribution.

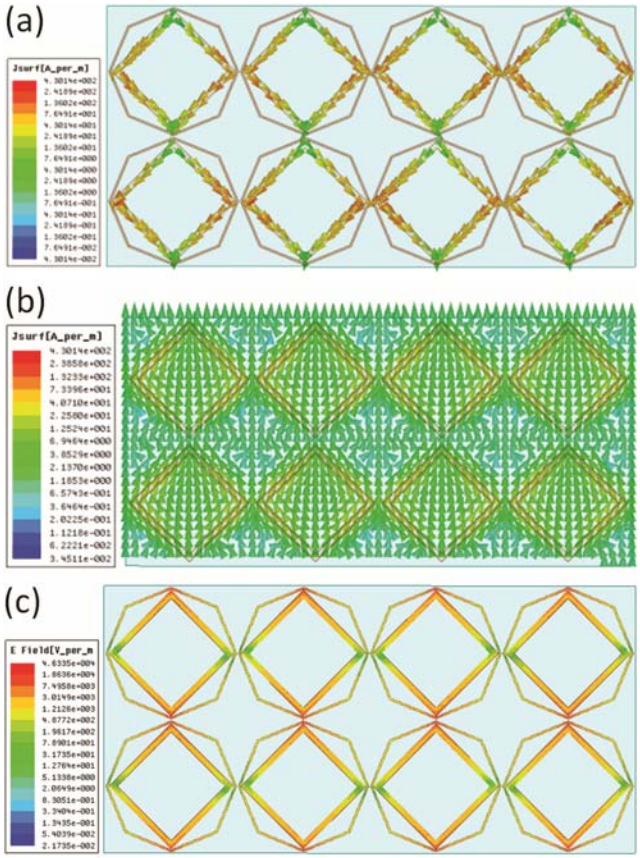

Fig. 5 — Calculated electrical parameters at high absorption frequency of 2.59 GHz: (a) Current distribution on top plane of the MMA, (b) current distribution on bottom plane of the MMA and (c) electric field distribution.

absorption is observed at 1.98 GHz frequency in contrast with the absorption at 2.59 GHz.

Consequently, the circulating current perpendicular to the incident EM wave excites magnetic response. While the distribution of electric field on the top metal surface of the MMA shows the existence of electric response. The electric field distributions for lower and higher frequencies are depicted in Figs 4-5(c), respectively. The field distribution graphs manifest that the electric field is strongly concentrated in the outer octagonal ring for lower absorption frequency, whereas it is strongly coupled to the inner rotated ring for the higher absorption frequency. Hence, it is clear that a strong coupling exists between the electric resonance and the incident EM wave on the top metal plane. Thus, by merely altering the geometrical parameters of the MMA electric and magnetic response could be changed to attain desired absorption at targeted frequency.

In addition, the proposed MMA design is supported by the polarization and oblique angle variation

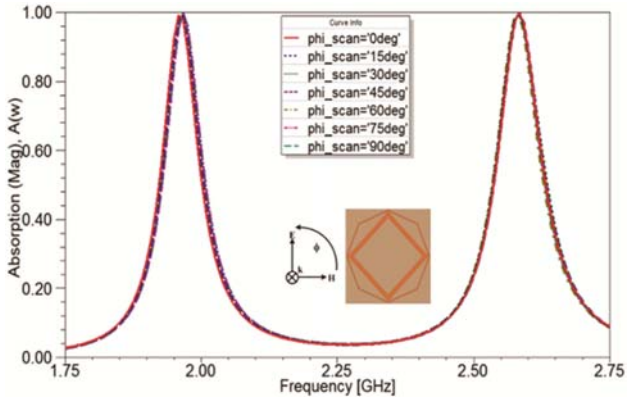

Fig. 6 — Simulated result depicting absorption efficiency response with respect to polarization angle variation.

graphs. The folding symmetry of the structure achieves the absorption efficiency of above 99% for all the polarization angles (ϕ) making proposed MMA design polarization independent and hence makes the design more practical. The absorption efficiency response with respect to variation in ϕ-angle is shown in Fig. 6. Practically, the variation of ϕ-angle is not

possible in waveguide measurement setup due to the closed measurement setup. However, the polarization insensitivity of structure could be measured practically by setting different orientation angles for the concentric CRRs and then fabricating each sample. The testing of differently oriented CRR samples would give the measured results for various ϕ-angles.

The effects of variation in oblique angle under TE and TM mode configuration are studied additionally. The respective numerical simulation results are illustrated in Fig. 7. It should be noted that for TE mode configuration when ϕ-angle and direction of electric field component of incident EM wave is kept constant while changing magnetic field by θ angle the absorption efficiency drops below 80% beyond 60° of θ-angle. Whereas, in case of TM mode configuration keeping ϕ-angle and direction of incident magnetic field constant the absorption efficiency of about 98% is achieve for all θ-angles with slight frequency shift in first band. This is caused due the octagonal geometry of the outer ring.

3.1 Absorption Mechanism

To further investigate the factors that influence the absorption efficiency, the electrical as well as physical parameters of the suggested MMA have been uniformly altered. At first the dielectric loss tangent has been varied from 0 to 100%. It is observed from Fig. 8 that as the loss tangent of the dielectric substrate is increased the losses present would increase eventually causing increase in the imaginary component of the impedance. This would cause reduction in absorption efficiency, however, with bandwidth enlargement. From this variation it could be concluded that loss tangent of a material has immense effect on the absorption bandwidth. Keeping this in mind, further investigation has been done by replacing the substrate of the proposed MMA with a novel material— neoprene rubber, having higher loss tangent[26] at microwave frequency than the originally selected FR4 dielectric substrate. Fig. 9 represents the numerical computation for the two materials. It is noted that the FWHM (full width at half maximum) bandwidth of the both absorption bands are in the range of ~4% in case of FR4 as substrate. On the

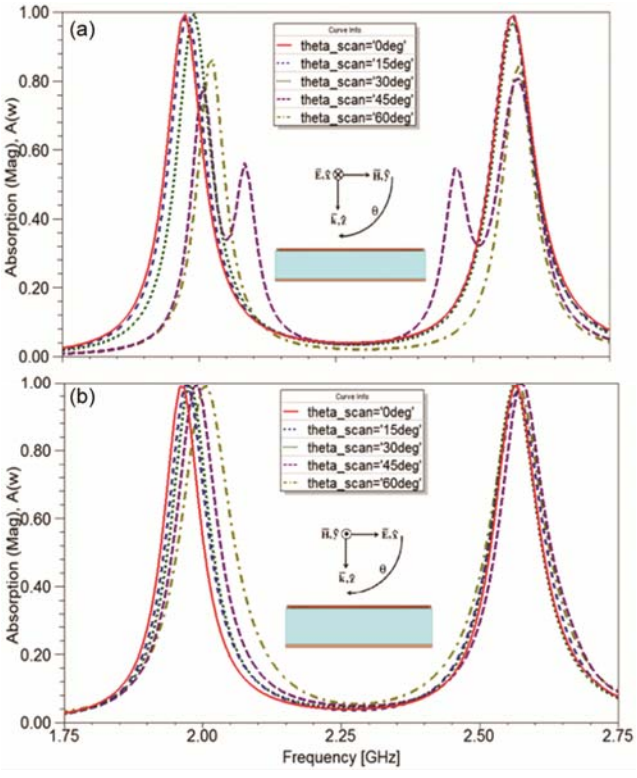

Fig. 7 — Simulated results for different oblique angle under: (a) TE mode and (b) TM mode.

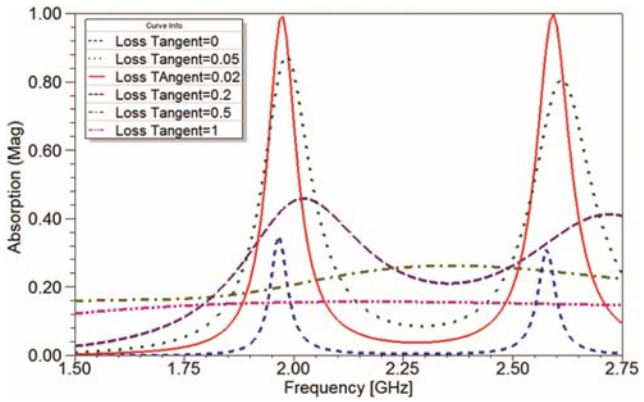

Fig. 8 — Simulated result depicting absorption efficiency response with respect to loss tangent variation.

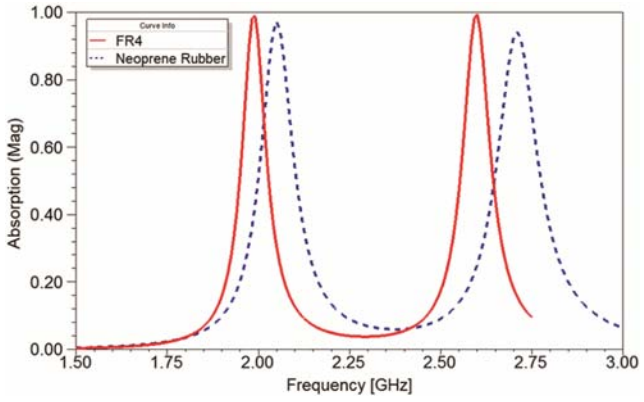

Fig. 9 — Comparative simulated result depicting absorption efficiency response for FR4 and neoprene rubber as substrate material.

other hand, with same geometrical parameters when FR4 is replaced with neoprene rubber, the FWHM bandwidth of both the absorption bands were obtained as ~5% with relative shift in frequencies and degraded absorption efficiency. It is possible to attain higher absorption band with wider bandwidth by optimizing the geometrical parameters with neoprene rubber as dielectric substrate.

Moreover, the dependency of absorption efficiency on number of unit cell in a MMA structure is illustrated in Fig. 10. The numerical computation is carried out with single, two and four unit cells and the simulated results are compared with the eight unit cell structure. The comparative graph illustrated in Fig. 10 depicts that when the EM wave is incidence on the structure with more number of unit cells, strong electric and magnetic response is induced which aids in achieving wide-angle stability and close matching of impedances. More number of unit cells could be added but it would require optimization in the geometrical parameter to achieve perfect absorption in the specified frequencies.

The proposed dual-band perfect MMA based on closed CRRs is compared with the recently reported similar designs[27,28]. The comparison is summarized in Table 1. Table 1 show the originality of the proposed work in terms of frequency selection in addition to the structure shape so that the proposed dual-band absorber could be practically implemented in shielding RF electronic components or systems against EMI/EMC interventions and also in energy harvester for absorbing ambient UMTS frequencies.

3.2 Fabrication, Setup and Measurement

The requirement of large scale sample (about 10λ) makes free space measurement method[29-31] impractical for testing proposed MMA. Hence the waveguide measurement method[32,33] is selected for the measurement of the proposed MMA. Another advantage of choosing latter method over former is simple measurement setup requirement. The proposed MMA was measured using WR430 waveguide connect to the Agilent N9912A vector network analyzer with RG142 Teflon coaxial cable. The measurement setup is displayed in Fig. 11(a). In this method, the sample size is same as that of the inner aperture of the waveguide. The final optimized MMA sample has 8-unit cell with each cell arranged periodically having interval of '*a*' mm as shown in Fig. 11(b). With this method return loss and insertion loss are calculated from VNA by placing sample inside the waveguide and covering it with a metal plate to reject any leaky waves.

The measured results are shown in Fig. 12. The measured return loss is obtained as 22.2 dB and 19.45 dB with absorption efficiency of 99.06% and 98.74% at 2 GHz and 2.56 GHz, respectively. The slight shift in the measured frequency was due to the presence of oblique incidence wave inside the standard waveguide rather than normal wave and also due to the fabrication tolerance and imperfection in material used. The normal wave has obliqueness which could be represented by the following expression:

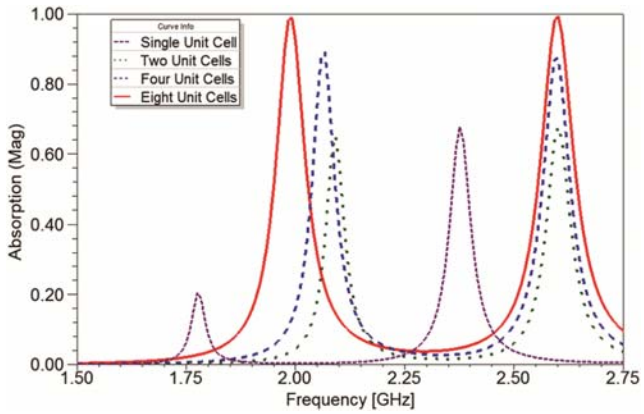

Fig. 10 — Simulated result depicting absorption efficiency response for different numbers of unit cell.

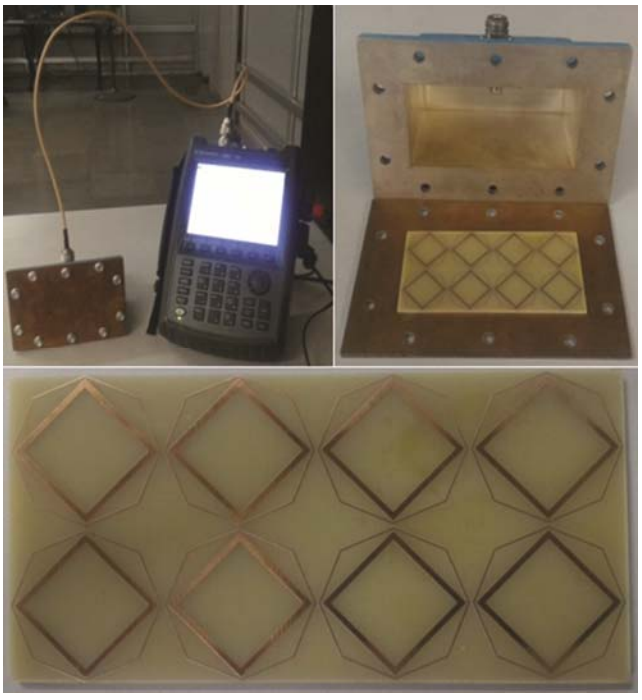

Fig. 11 — (a) Waveguide Measurement Setup and (b) fabricated sample consisting of 8-unit cells.

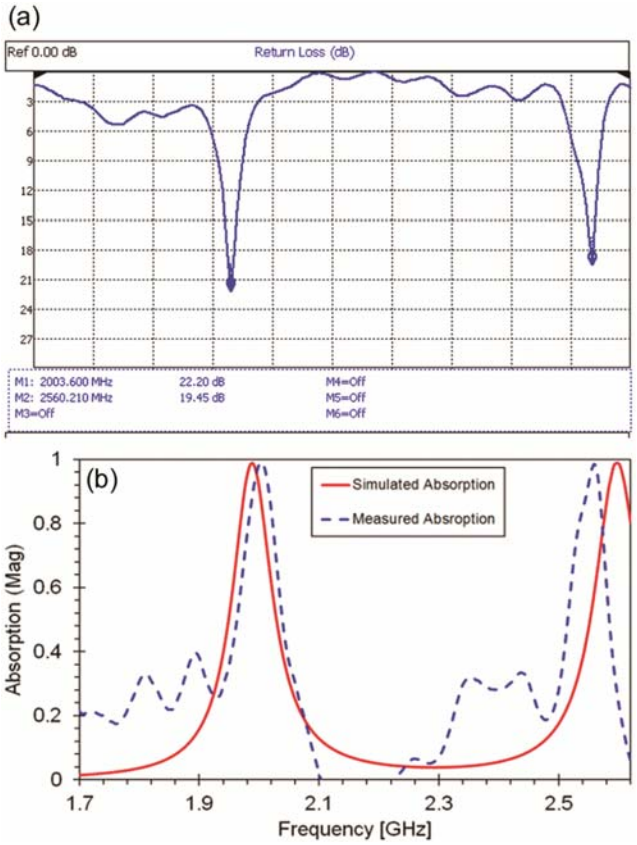

Fig. 12 — Measured results: (a) Return loss and (b) comparison of simulated and measured absorption.

$$\theta = sin^{-1}(\lambda/2a) \quad \ldots (2)$$

The small ripples in the measured results could possibly be eliminated by extending the waveguide by adding additional quarter more transmission line.

4 Conclusions

The design, fabrication and measurement of dual-band perfect metamaterial based absorber with polarization stability and wide incidence angle is presented in this article. The absorber structure was measured with waveguide measurement technique achieving measured absorption of 99.06% and 98.47% at 2 GHz and 2.56 GHz, respectively. Numerical calculations are very close to the measured result. Based on simulation results the structure is considered as highly polarization insensitivity with good absorption of TE-mode wave up to 60° of obliqueness and very high absorption for all TM-mode waves. In this article, a method has been described to obtain polarization variation practically in case of waveguide measurement method and the numerical results for FR4 and novel substrate—neoprene rubber have been presented.

References

1 Veselago V G, *Soviet Physics Uspekhi*, 10 (1968) 509.
2 Smith D R, Padilla W J, Vier D C, Nemat-Nasser S C & Schultz S, *Physical Review Letters*, 84 (2000) 4184.
3 Shelby R A, Smith D R & Schultz S, *Science*, 292 (2001) 77.
4 Fang N & Zhang X, *Applied Physics Letters*, 82 (2003) 161.
5 Zhang X & Liu Z, *Nature Materials*, 7 (2008) 435.
6 Upadhyaya T K, Kosta S P, Jyoti R & Palandoken M, *Optical Engineering*, 53 (2014) 107104.
7 Upadhyaya T K, Kosta S P, Jyoti R & Palandöken M, *International Journal of Microwave And Wireless Technologies*, 8 (2016) 229.
8 Schurig D, Mock J J, Justice B J, Cummer S A, Pendry J B, Starr A F & Smith D R, *Science*, 314 (2006) 977.
9 Sabah C, Dincer F, Karaaslan M, Unal E, Akgol O & Demirel E, *Optics Communications*, 322 (2014) 137.
10 Chen T, Li S & Sun H, *Sensors*, 12 (2012) 2742.
11 Unal E, Dincer F, Tetik E, Karaaslan M, Bakir M & Sabah C, *Journal of Materials Science: Materials in Electronics*, 26 (2015) 9735.
12 Bakir M, Karaaslan M, Dincer F, Akgol O & Sabah C, *International Journal of Modern Physics B*, 30 (2016) 1650133.
13 Caloz C & Itoh T, *John Wiley & Sons*; 2005 Nov 22.
14 Li M, Yang H L, Hou X W, Tian Y & Hou D Y, 108 (2010) 37.
15 Landy N I, Sajuyigbe S, Mock J J, Smith D R & Padilla W J, *Physical review letters*, 100 (2008) 207402.
16 Tuong P V, Park J W, Rhee J Y, Kim K W, Jang W H, Cheong H & Lee Y P, *Applied Physics Letters*, 102 (2013) 081122.
17 Bhattacharyya S, Ghosh S & Vaibhav Srivastava K, *Journal of Applied Physics*, 114 (2013) 094514.
18 Wang G D, Chen J F, Hu X, Chen Z Q & Liu M, *Progress In Electromagnetics Research*, 145 (2014) 175.
19 Wang B X, Zhai X, Wang G Z, Huang W Q & Wang L L, *IEEE Photonics Journal*, 7 (2015) 1.
20 Ramya S & Srinivasa Rao I, *Progress In Electromagnetics Research M*, 50 (2016) 23.
21 Sood D, *Indian Journal of Radio & Space Physics (IJRSP)*, 45 (2016) 57.
22 Sharma S K, Ghosh S, Srivastava K V & Shukla A, *Microwave and Optical Technology Letters*, 59 (2017) 348.
23 Xie T, Chen Z, Ma R & Zhong M, *Optics Communications*, 383 (2017) 81.
24 Kim Y J, Hwang J S, Yoo Y J, Khuyen B X, Chen X & Lee Y, *Current Applied Physics*, 2017 Jun 20.
25 Smith D R, Vier D C, Koschny T & Soukoulis C M, *Physical review E*, 71 (2005) 036617.
26 Ahmad Z, Polymer Dielectric Materials. In *Dielectric Material* (InTech), 2012.
27 Wang W, Chen Y, Yang S, Zheng X & Cao Q, *Journal of Electromagnetic Waves and Applications*, 29 (2015) 2080.
28 Sood D & Tripathi C C, *Journal of Electromagnetic Waves and Applications*, 31 (2017) 394.
29 Nguyen T T & Lim S, *Scientific Reports*, 7 (2017)14814.
30 Chaurasiya D, Ghosh S, Bhattacharyya S & Srivastava K V, *Microwave and Optical Technology Letters*, 57 (2015) 697.
31 Ghosh S, Bhattacharyya S & Srivastava K V, *IET Microwaves, Antennas & Propagation*, 10 (2016) 850.
32 Li L, Yang Y & Liang C, *Journal of Applied Physics*, 110 (2011) 063702.
33 Zhai H, Zhan C, Liu L & Zang Y, *Electronics Letters*, 51 (2015) 1624.